Declassified 1-10-46

CONFIDENTIAL

OFFICE OF SCIENTIFIC RESEARCH & DEVELOPMENT
NATIONAL DEFENSE RESEARCH COMMITTEE
DIVISION SIX - SECTION 6.1

FORCE TESTS OF CONCRETE PRACTICE BOMBS M38A2 PRACTICE BOMB AN-M43 G.P. 500LB. BOMB AN-M56 L.C. 4000LB. BOMB

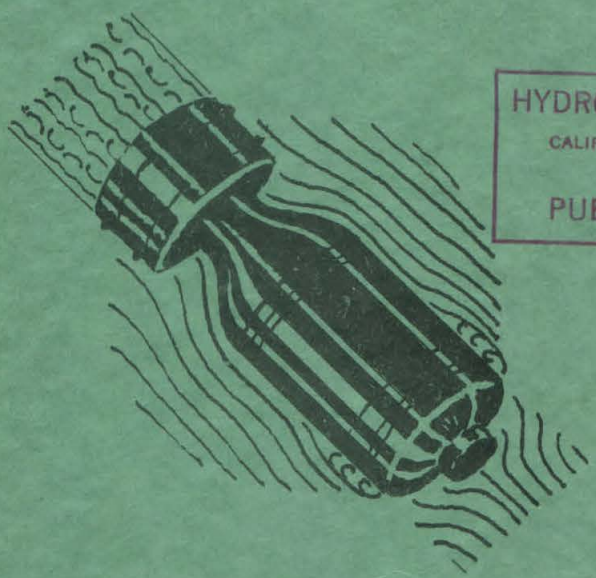

THE HIGH SPEED WATER TUNNEL
CALIFORNIA INSTITUTE OF TECHNOLOGY.
PASADENA, CALIFORNIA

SECTION Nº 6.1 - sr 207-2245
LABORATORY Nº ND-32

CONFIDENTIAL

~~CONFIDENTIAL~~

OFFICE OF SCIENTIFIC RESEARCH AND DEVELOPMENT
NATIONAL DEFENSE RESEARCH COMMITTEE
DIVISION SIX – SECTION 6.1

FORCE TESTS

OF

CONCRETE PRACTICE BOMBS
M38A2 PRACTICE BOMB
AN–M43 G.P. 500 LB. BOMB
AN–M56 L.C. 4000 LB. BOMB

ROBERT T. KNAPP

OFFICIAL INVESTIGATOR

THE HIGH SPEED WATER TUNNEL
AT THE
CALIFORNIA INSTITUTE OF TECHNOLOGY
HYDRODYNAMICS LABORATORY
PASADENA, CALIFORNIA

Section No. 6.1-sr207-2245

Laboratory No. ND-32

Report Prepared by
Robert M. Peabody
Hydraulic Engineer

August 14, 1945

~~CONFIDENTIAL~~

TABLE OF CONTENTS

FORCE TESTS
OF
CONCRETE PRACTICE BOMBS
M38A2 PRACTICE BOMBS
AN-M43 G.P. 500 LB. BOMB
AN-M56 L.C. 4000 LB. BOMB

INTRODUCTION

This report covers model tests in the High Speed Water Tunnel and Polarized Light Flume of the Hydrodynamics Laboratory at the California Institute of Technology on the following aircraft bombs for use against land targets and surface targets on water:

Concrete Practice Bombs

(a) with large fin box tail

(b) with small fin box tail

(c) with drum type tail

M38A2 Practice Bomb

AN-M43 G.P. 500 lb. Bomb

AN-M56 L.C. 4000 lb. Bomb

The tests were authorized under Project OD 99.

Tests were made on two-inch diameter models in the High Speed Water Tunnel to determine the hydrodynamic forces (drag, cross force, and moment) under steady state conditions. No tests were made to determine the damping forces. The test results apply only to velocities below the velocity of sound.

Tests were made in the Polarized Light Flume to give a visual indication of the streamline patterns in steady flight.

A comparison is made of the results of the Water Tunnel tests with tests previously made on models of the same bombs at the Wright Field Wind Tunnel(1).

(1) "Aerodynamic Tests of Finned Projectiles Performed in the Twenty Foot Wind Tunnel at Wright Field" by A. C. Charters and J. L. Kelley, Report No. 471, 16 June 1944, Ordnance Research Center Project No. 3986.

SUMMARY AND CONCLUSIONS

Table I shows, for comparison, the principal hydrodynamic characteistics shown by the tests.

TABLE I

COMPARISON OF HYDRODYNAMIC CHARACTERISTICS

	Concrete Practice Bombs			M38A2	AN-M43	AN-M56
	Large Box Tail CPCA-1	Small Box Tail CPCA-2	Drum Tail CPCA-3	100 lb Pract Bomb	GP 500 lb Bomb	LC 4000 lb Bomb
Drag coefficient, C_D						
At zero yaw	0.285	0.250	0.240	0.270	0.220	0.287
At $\pm 6^\circ$ yaw	0.315	0.305	0.290	0.295	0.260	0.325
Cross force coefficient, C_C						
C_C per degree, 0 to $+1^\circ$ yaw	0.062	0.065	0.050	0.055	0.060	0.056
C_C at $+6^\circ$ yaw	0.450	0.460	0.335	0.440	0.380	0.355
Moment coefficient, C_M						
C_M per degree, 0 to $+1^\circ$	-0.008	-0.006	-0.009	-0.008	-0.009	-0.005
C_M at $+6^\circ$ yaw	-0.085	-0.081	-0.058	-0.074	-0.065	-0.041
Center of pressure eccentricity, e, at $+6^\circ$ yaw	-0.189	-0.176	-0.173	-0.168	-0.171	-0.115
Reynolds number x 10^6						
Model in water at 32 ft/sec	2.4	2.4	2.8	2.9	2.0	1.7
Prototype in air at 600 ft/sec	12	12	14	14	18	35

The comparison is with the box tails so oriented that the sides of the fin box are at 45 degrees with the yaw plane.

Of the three concrete practice bombs, that with the drum-type tail (CPCA No. 3) showed the greatest static stability near zero yaw, and also showed a somewhat lower drag than the others. If the shroud of the drum-type tail could be slightly increased in diameter, it is believed that still greater stability would result.

The M38A2 Practice Bomb has characteristics closely comparable to the concrete practice bombs with box tails.

The AN-M56 4000 lb. Bomb shows considerably higher drag and less static stability than the An-M43 500 lb. Bomb. The higher drag can be attributed to the steep slope of the afterbody of the 4000 lb. Bomb, and the lower stability to the location of the

box tail so close to the afterbody that it lies directly in the *afterbody wake* (see Figure 20).

All of the models vibrated at a speed of 32 ft/sec in the water tunnel. The vibration caused failure of the tail supports on each of the concrete practice bomb models. The vibration was particularly severe on the model of the 4000 lb. bomb. At 32 ft/sec the fin reinforcing struts on the model failed, and at 55 ft/sec one side of the box tail collapsed.

Drag measurements at velocities higher than 32 ft/sec were unsatisfactory on account of the vibration.

Failure of the models does not, of course, indicate corresponding failures on the prototype bombs. However, the failures do show that forces of considerable magnitude act on the tails of the bombs at high velocities.

Comparison with the tests previously made in the Wright Field Wind Tunnel on prototype size models of the Concrete Practice Bombs, the 500 lb. Bomb, and the 4000 lb. Bomb showed close agreement for the 500 lb. and 4000 lb. Bombs.

DESCRIPTION OF BOMBS AND MODELS

Figure 1 shows, to the same scale, the outlines of the prototype bombs. The principal dimensions of the prototypes and models are given in Table II.

TABLE II

PRINCIPAL PROTOTYPE DIMENSIONS

	Concrete Practice Bombs			M38A2	AN-M43	AN-M56
	Large Box Tail CPCA-1	Small Box Tail CPCA-2	Drum Tail CPCA-3	100 lb Pract. Bomb	GP 500 lb Bomb	LC 4000 lb Bomb
Maximum diameter, in.	8	8	8	8	14	34
Overall length, in.	38.50	38.50	45.50	47.50	58.14	116.06
Body length, in.	30.10	30.10	30.10	40.66	48.33	96.12
Afterbody taper, deg. from long. axis	10.3	10.3	10.3	15.7	24	30
Side of fin box, in.	6.00	4.75	8(dia)	6.00	7.60	22.56
Max. span of fins, in.	11.00	11.00	8(dia)	10.77	18.94	47.62
Weight, pounds	103.25	103.25	104	100	508	4200
Nose tip to C.G., in.	14.75	14.75	15.50	18.15	24.00	49.20
Scale ratio, prototype to model	4:1	4:1	4:1	4:1	7:1	17:1

Details of the projectiles covered by this report will be found on the following reference drawings:

Concrete Practice Bombs
Concrete Products Co. of America, Drawings B6, B7, B8

M38A2 Practice Bomb
U. S. Ordnance Department Drawing 82-O-23

AN-M43 G.P. 500 lb. Bomb
U. S. Ordnance Department Drawing 82-O-27

AN-M56 L.C. 4000 lb. Bomb
U. S. Ordnance Department Drawing 82-O-55

The noses of the concrete practice bombs and the M38A2 Practice Bomb are identical and approximate very closely a 1.28 caliber x 56 degree spherogive. The nose of the 500 lb. Bomb is a compound ogive of 1.26 caliber followed by a radius of 0.76 caliber, and terminating in a blunt nose tip. The nose of the 4000 lb. Bomb is an ogive of 0.94 caliber, terminating in a conical end of 88° included angle and with a blunt nose tip.

All of the models are two inches in diameter, and as to external dimensions are accurate scale reproductions of the prototypes except that nose and tail fuzes are omitted. The models are made of brass or bronze and stainless steel.

TEST PROCECURE - FORCE TESTS

The hydrodynamic characteristics determined by the model tests are expressed in terms of drag, cross force, and moment coefficients calculated from the observed forces and moments. The symbols and definitions of the coefficients are given in the appendix.

For the force and moment measurements the model is mounted on a shielded spindle in the working section of the water tunnel. The spindle, to which the model is rigidly attached, is extended outside the working section and connected to balances which measure the forces and moments. The shield which surrounds the mounting spindle in the working section is streamlined and extends from the bottom of the working section to within a few thousandths of an inch of the model, thus protecting the spindle from the tunnel flow. To compensate for interference between the shield and the model, each series of tests is repeated with an image shield extending from the top of the working section to the same clearance from the model as the spindle shield. The image shield is a mirror duplicate of the spindle shield.

A tare or shield interference correction is then applied in accordance with standard wind tunnel practice as follows:

$$F = F_o - (F_w - F_o)$$

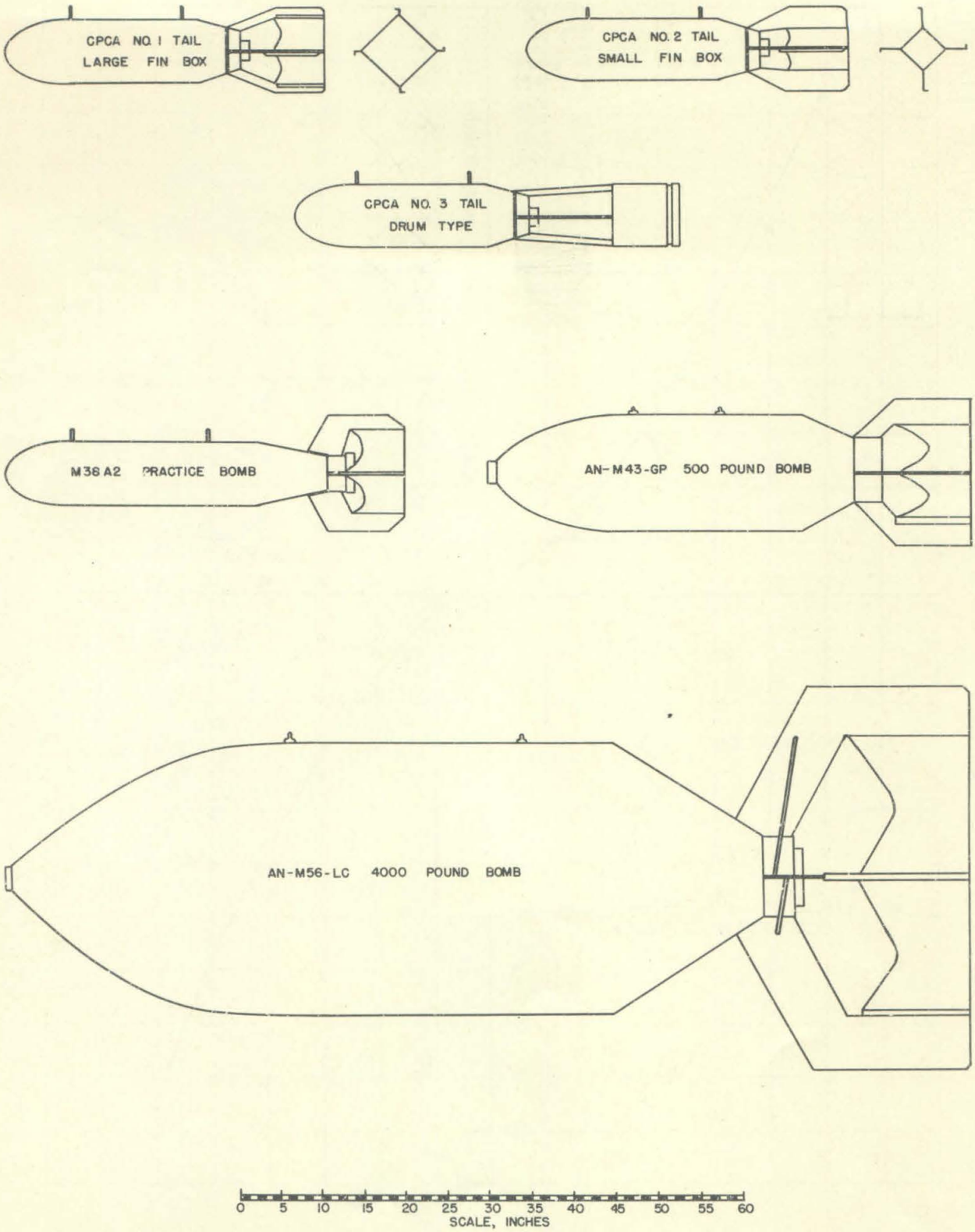

FIG. 1 — OUTLINE DRAWINGS OF AIRCRAFT BOMBS

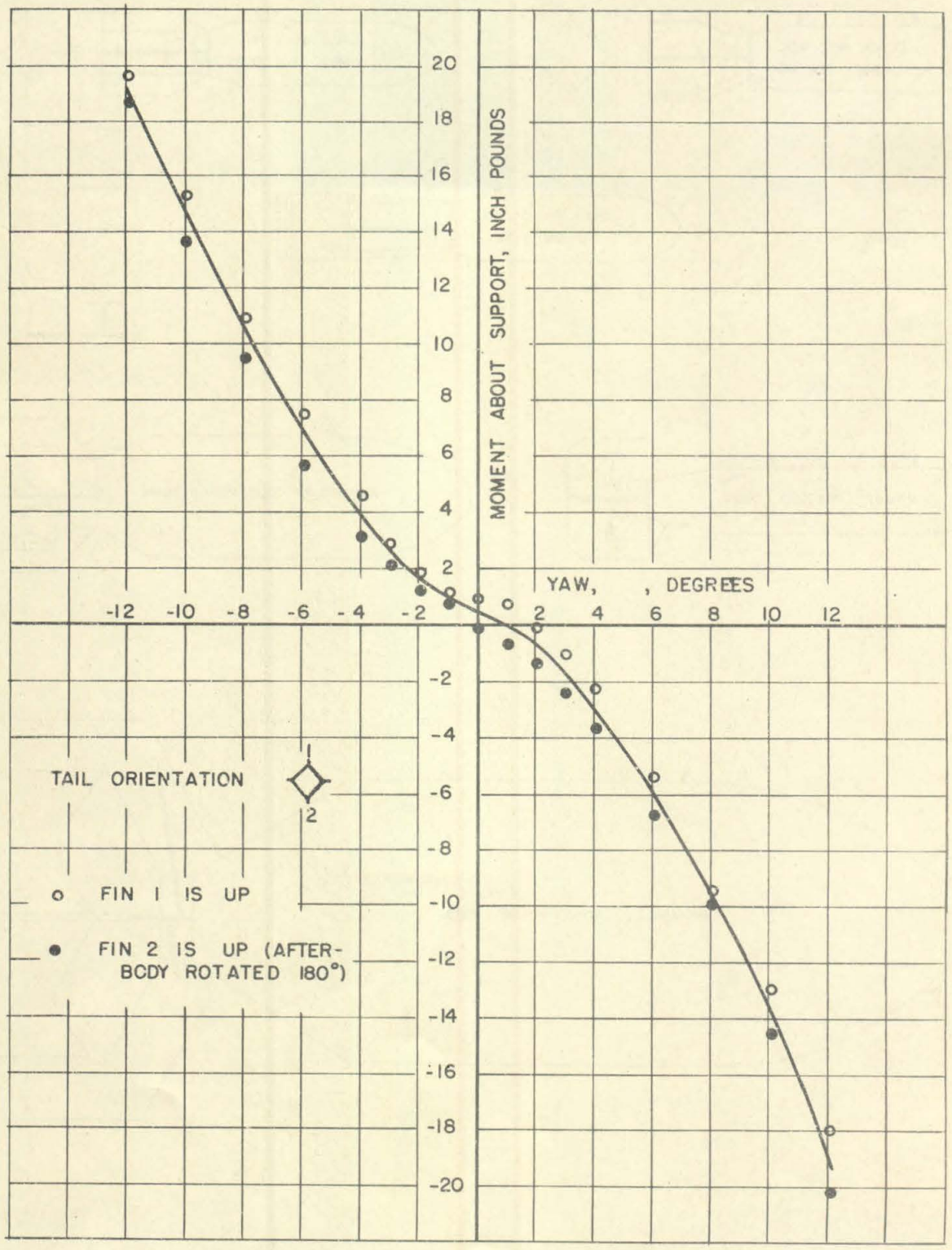

FIG. 2 — EFFECT OF ASYMMETRY ON MOMENT

where

F = the corrected force or moment

F_o = the measured force or moment with the spindle shield only

F_w = the measured force or moment with both the spindle and image shield

EFFECT OF ASYMMETRY

None of the bombs is completely symmetrical about any plane through the longitudinal axis. The asymmetry is due mainly to the construction of the tails; also to the effect of the supporting lugs and to accidental asymmetry in construction. The result of asymmetry is that the curves of cross force and moment vs. yaw do not pass through zero at zero yaw. This effect is typically illustrated by Figure 2, in which the observed moments in inch-pounds (after shield interference correction) are shown for a range of positive and negative yaws and for orientations of the bomb tail 180° apart with respect to the yaw plane. If, so to speak, the asymmetry itself were symmetrical, the two sets of points for opposite orientations would be expected to give moment-yaw curves passing on opposite sides of and about equidistant from the intersection of the coordinate axes. As can be seen from the figure, this is not the case. The smooth curve of the figure is drawn through moment values which are the average of the values given by the two 180° apart orientations. To approximate the moment curve of a completely symmetrical bomb, the portion of the averaged curve for negative yaws and positive moments is replotted for corresponding positive yaws and negative moments and averaged with the curve already plotted for positive yaws. The resulting curve passes through the intersection of the coordinate axes, and values obtained from this curve were used in calculating the coefficients.

All of the models tested showed the effect of asymmetry to a greater or less degree. The asymmetry indicated in Figure 2 is for the Concrete Practice Bomb with the large fin box tail (CPCA No. 1), which appeared to have a greater degree of asymmetry than any of the other models.

The force and moment coefficients for all of the models tested were calculated from force and moment curves faired and averaged by the procedure above outlined. The resulting coefficient curves, therefore, represent the characteristics of a completely symmetrical projectile.

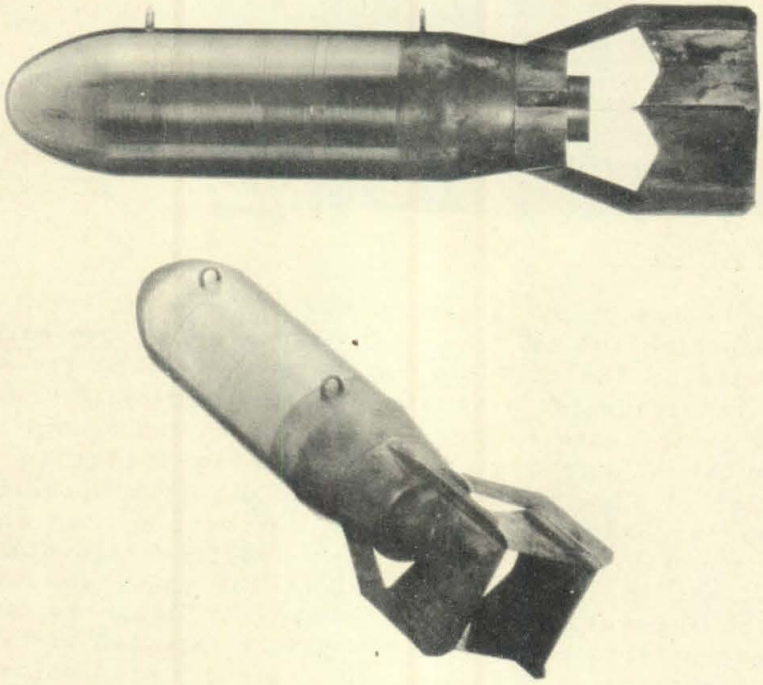

FIG. 3 – MODEL OF CONCRETE PRACTICE BOMB, CPCA NO. 1
(LARGE FIN BOX)

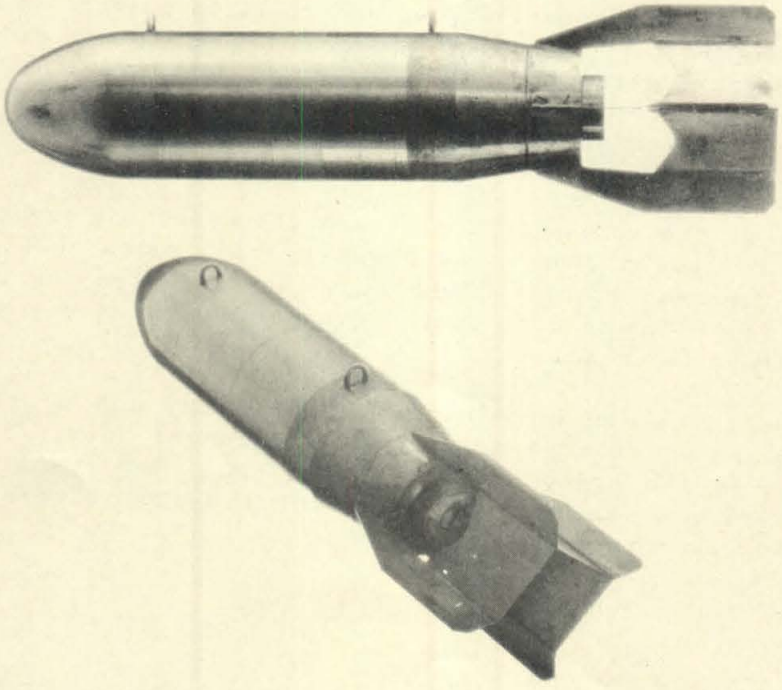

FIG. 4 – MODEL OF CONCRETE PRACTICE BOMB, CPCA NO. 2
(SMALL FIN BOX)

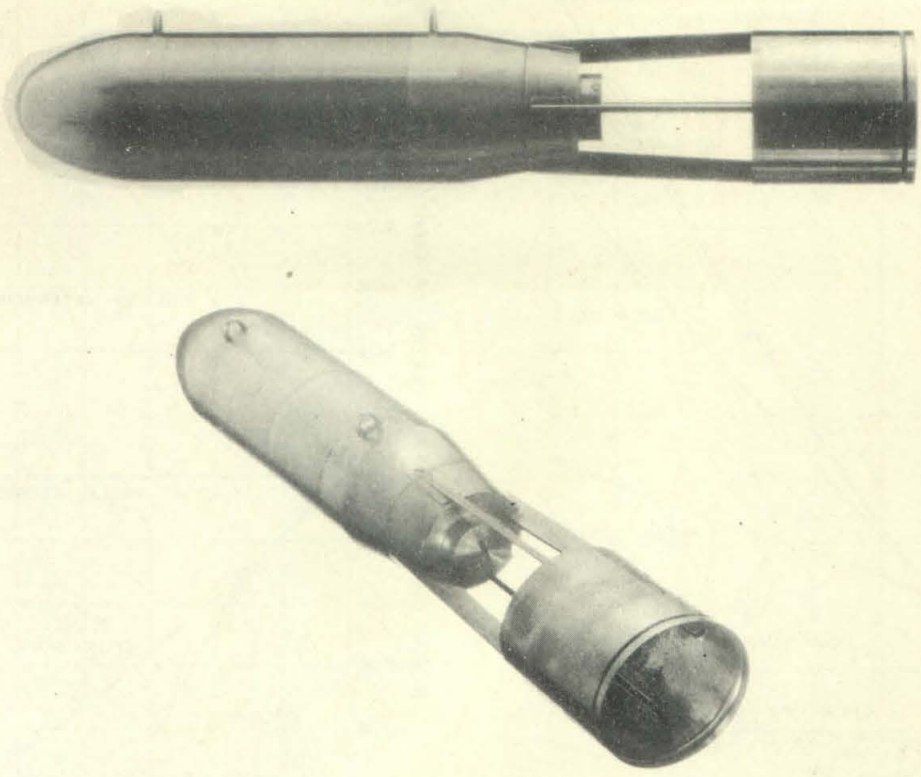

FIG. 5 — MODEL OF CONCRETE PRACTICE BOMB, CPCA NO. 3 (DRUM TYPE)

CONCRETE PRACTICE BOMBS

The Concrete Practice Bombs were designed by the Concrete Products Company of America. The bodies of the three bonbs are identical, formed of solid concrete, the variation being in the construction of the tails, which are fabricated from steel plates.

Figures 3, 4, and 5 are photographs of the three models.

The CPCA No. 1 and No. 2 Tails are identical except for the dimensions of the square, open-ended box which forms the principal part of the tail. On the CPCA No. 1 Tail this box is 6 inches x 6 inches, and on the CPCA No. 2 Tail it is 4-3/4 inches x 4-3/4 inches. On both tails there are fins extending outward from the corners of the box.

The CPCA No. 3 Tail is called the "drum type". The tail is a cylindrical shroud ring supported from the afterbody on four U-shaped steel members. The shroud ring or drum is the same diameter as the cylindrical body of the bomb, and the length of the ring is equal to the diameter. The CPCA No. 3 Tail extends seven inches farther aft than the other two.

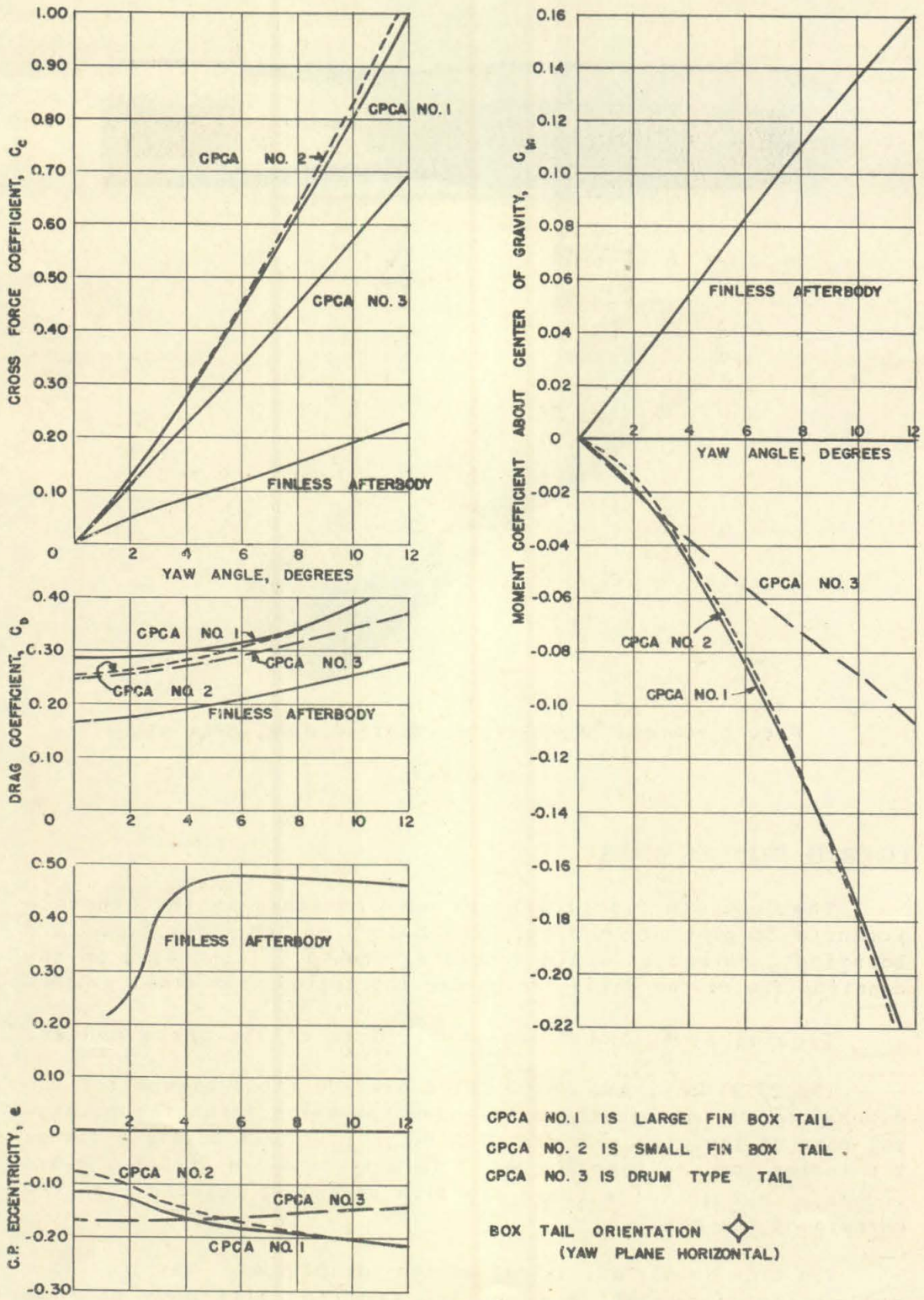

FIG. 6 – CONCRETE PRACTICE BOMBS

COMPARISON OF FORCE AND MOMENT COEFFICIENTS

Figure 6 shows a comparison of the drag, cross force, and moment coefficients of the three CPCA tails, and also shows the coefficients of the finless afterbody.

The significant differences between the three tails appear to be the following:

1. The drag is highest for the large fin box tail (CPCA No. 1). The drum-type tail (CPCA No. 3) has the lowest drag, but only slightly less than the small fin box tail (CPCA No. 2). For all three bombs the drag increases with yaw.

2. The cross force is almost the same at all yaws for the large and small fin box tails, and is considerably less for the drum-type tail than for the box tails.

3. The static stability at small yaws (less than 3°) is greater for the drum-type tail than for the box tails, as measured by the center-of-pressure eccentricity curves and the slope of the moment coefficient curve. At yaws greater than about 3°, the box-type tails show a greater restoring moment.

4. The finless afterbody, as would be expected, is statically unstable.

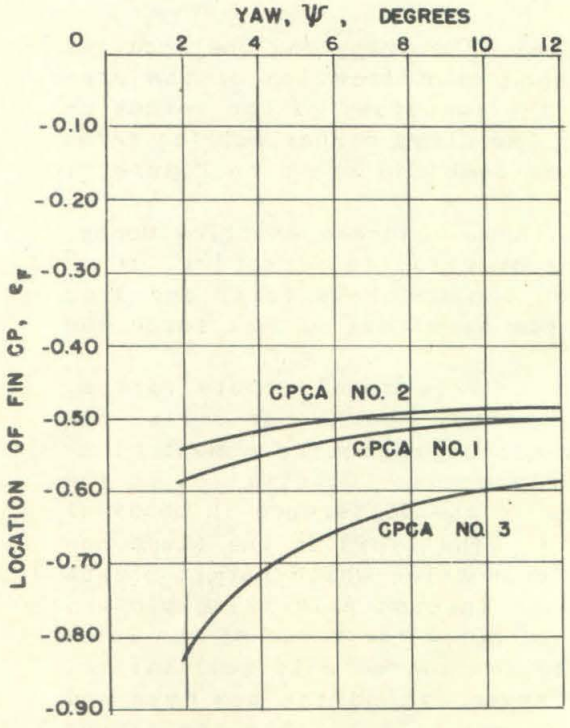

FIG. 7 – CONCRETE PRACTICE BOMBS
LOCATION OF RESULTANT OF FIN FORCES
AFT OF C.G., AS FUNCTION OF YAW

The coefficient curves of the finless afterbody offer a means of locating the resultant of the forces acting on the fins alone. Let C_{CH} and C_{MH} denote the cross force and moment coefficients of the finless afterbody. C_C and C_M are the cross force and moment coefficients of the bomb with fins. Then $(C_C - C_{CH})$ and $(C_M - C_{MH})$ represent the cross force and moment coefficients of the fins alone (including forces developed by interference between body and fins). Omitting the effect of drag, which is negligible at small yaws, the location on the projectile axis of the resultant of the fin force is

$$e_F = \frac{C_M - C_{MH}}{C_C - C_{CH}}$$

where

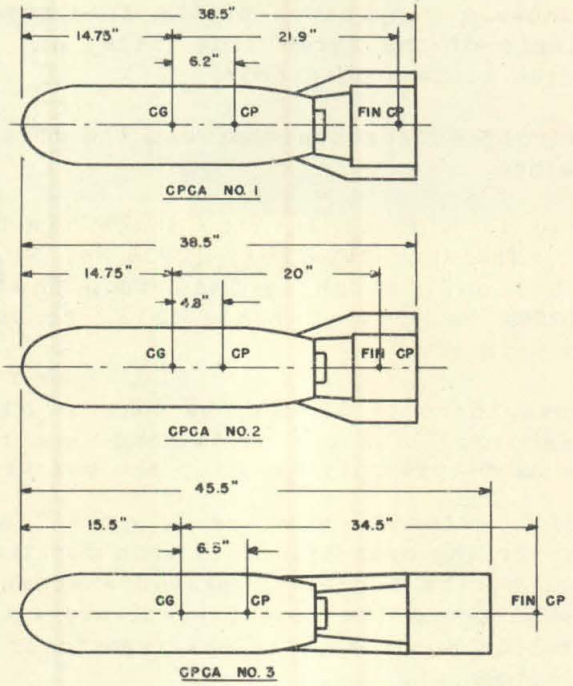

FIG. 8 – CONCRETE PRACTICE BOMBS
LOCATION OF CENTERS OF PRESSURE OF BODY AND FINS TOGETHER (CP) AND OF FINS ALONE (CP FINS) AT 3° YAW

e_F is the distance between the center of gravity and the location of the fin force resultant expressed as a fraction of the projectile lengths. The location of the resultant of the forces on the fins alone has been computed in the above manner for the three variations of the Concrete Practice Bomb and shown on Figure 7.

Figure 8 shows, to scale, the three concrete practice bombs, with the location of the center of gravity, the location, at 3° yaw, of the resultant normal force due to cross force and drag on the bomb as a whole (CP), and the resultant normal force due to the fins alone (fin CP).

It is to be noted that the fin CP is considerably farther aft on the drum-type tail than on either of the box tails, although, as shown by Figure 6, the static restoring moment at 3° yaw is nearly the same for all three bombs. Observation in the Polarized Light Flume offers a clue to the difference in behavior of the box-type and drum type tails. The fluid in the flume has asymmetrical physical and optical properties which permit observation of the flow lines when viewed through polarizing plates. The velocities in the light flume are below the range of the water tunnel tests and the pattern can be considered only qualitative. Figures 9 and 10 show the flow pattern around the box-type and drum type tails. From Figure 10 it can be seen that the shroud ring of the drum-type tail (CPCA No. 3) is very close to the eddies formed in the wake of the rather blunt afterbody. The fins

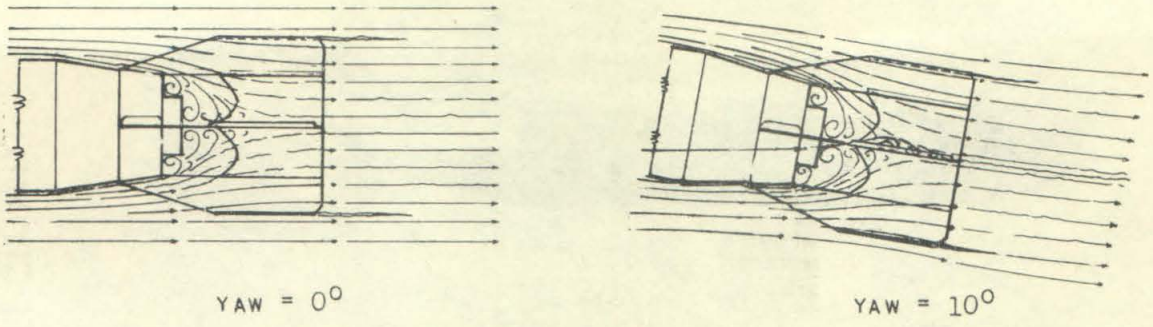

YAW = 0° YAW = 10°

FIG. 9 – FLOW PATTERNS AT 0° AND 10° YAW AROUND AFTERBODY AND TAIL CONCRETE PRACTICE BOMB CPCA NO. 2 (SMALL FIN BOX)

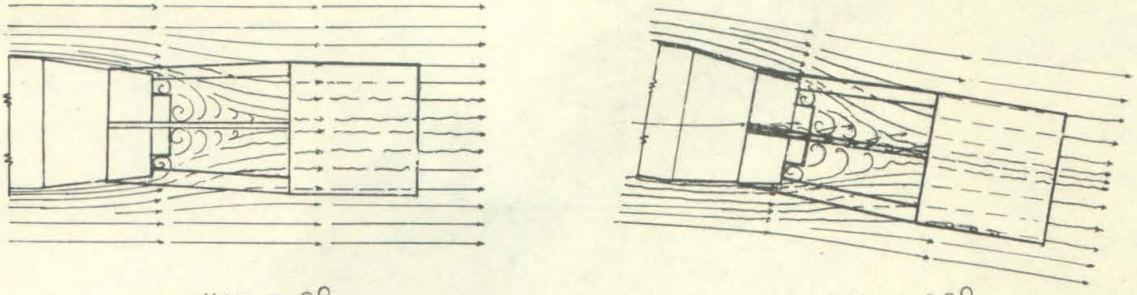

YAW = 0° YAW = 10°

FIG. 10 – FLOW PATTERNS AT 0° AND 10° YAW AROUND AFTERBODY AND FINS CONCRETE PRACTICE BOMB CPCA NO. 3 (DRUM TYPE)

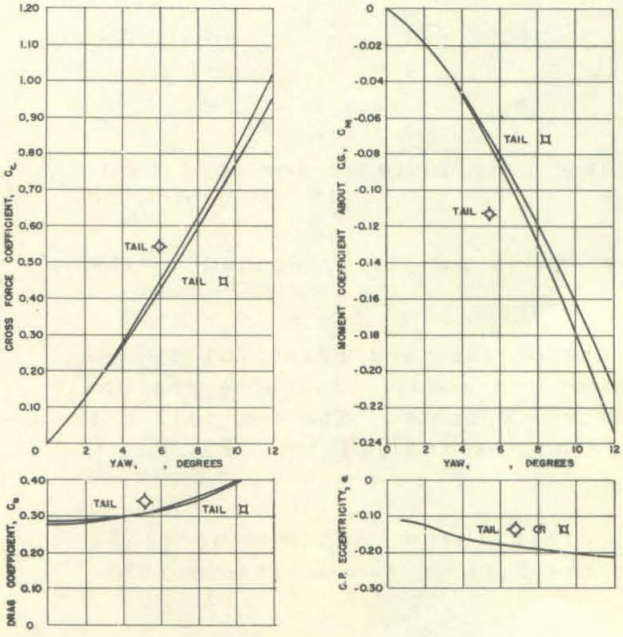

FIG. 11 – CONCRETE PRACTICE BOMB CPCA NO. 1: EFFECT OF TAIL ORIENTATION

which project from the corners of the box tails have a span greater than the shroud ring of the drum tail and extend into the almost undisturbed fluid. The cross force due to the previously undisturbed fluid acting on the wider fins probably accounts for the greater cross force (see Figure 6) on the bombs with the box tails.

Figure 11 shows the effect of the orientation of the box tail of CPCA No. 1 on the force and moment coefficients. The effect is seen to be negligible except at large yaws. The same negligible effect was observed in tests of the CPCA No. 2 and No. 3.

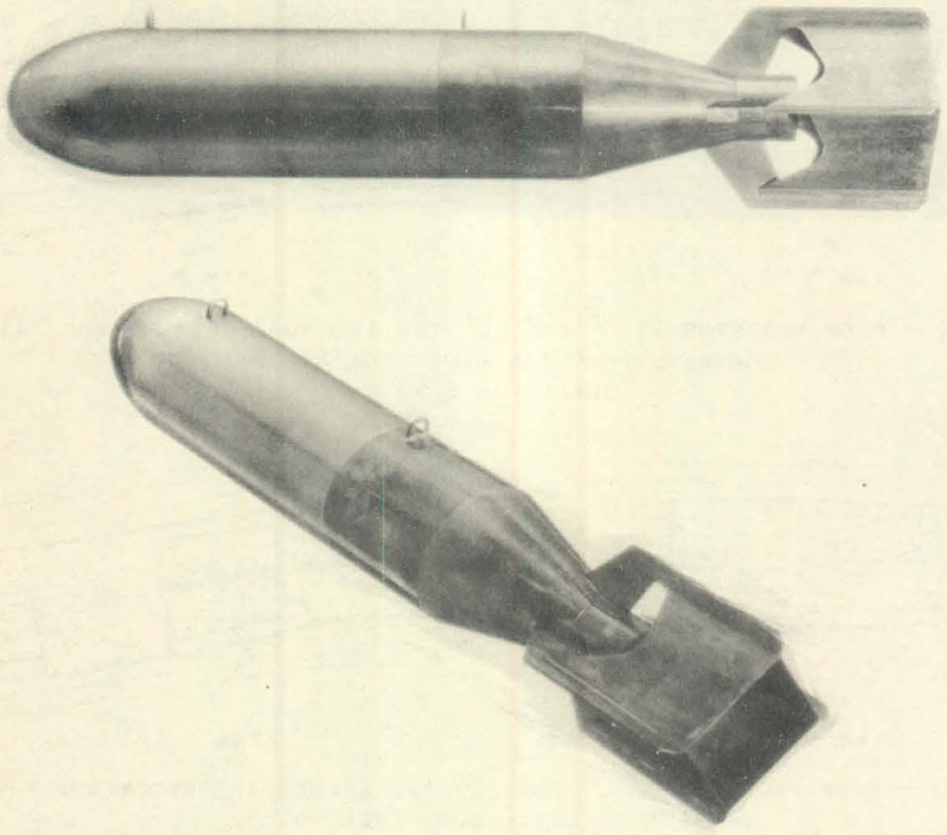

FIG. 12 – MODEL OF M38A2 – 100 LB. PRACTICE BOMB

M38A2 – 100 LB. PRACTICE BOMB

This is a bomb with sheet metal body designed for sand loading to weight at point of use.

It is furnished with a sheet metal box tail, welded to the afterbody.

Figure 1 and Table II give the outline and principal dimensions. Figure 12 shows two views of the model. The nose profile is the same as on the Concrete Practice Bombs. The box tail has approximately the same dimensions as the tail of the CPCA No. 1 Concrete Practice Bomb.

Figure 13 shows the drag, cross force, and moment coefficients for the M38A2 Bomb with the tail in two positions relative to the yaw plane.

Figure 14 shows the flow pattern around the afterbody and tail of the M38A2 Bomb. It shows the same characteristics as Figure 9 for the CPCA No. 2 tail.

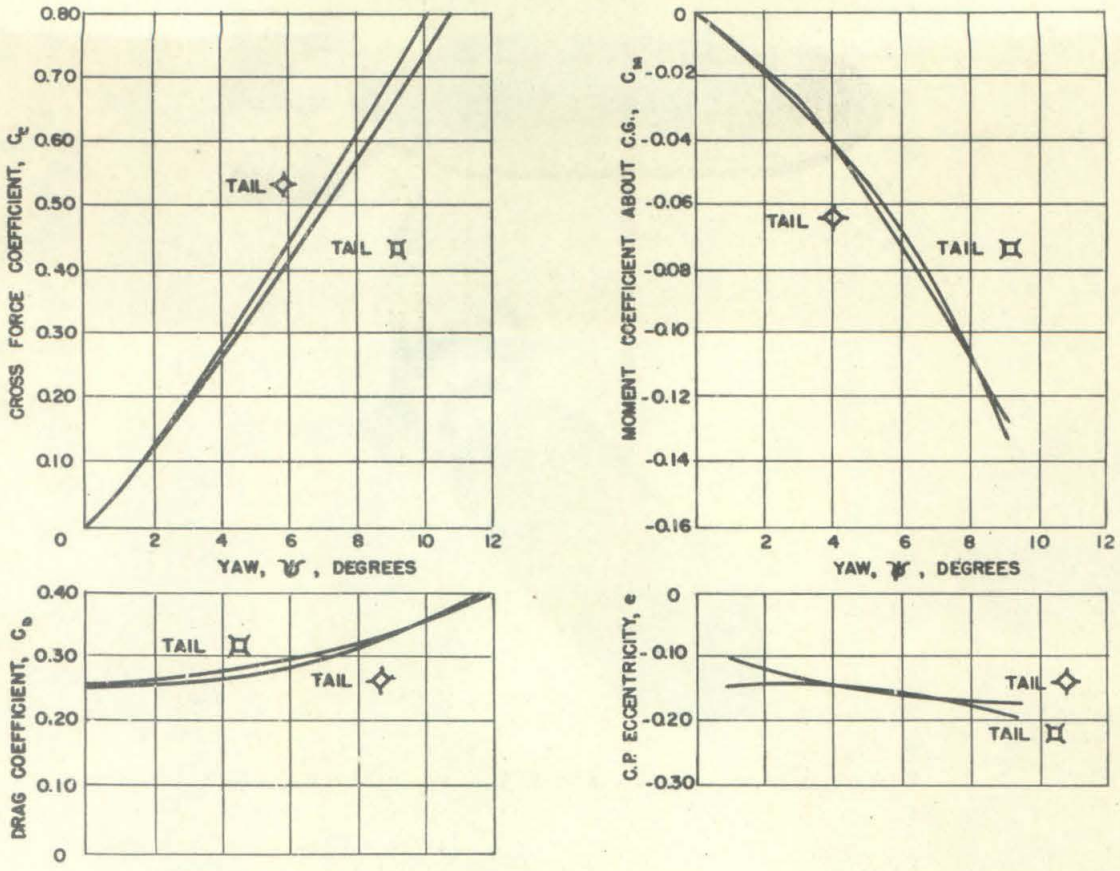

FIG. 13 – M38A2 PRACTICE BOMB

FORCE AND MOMENT COEFFICIENTS

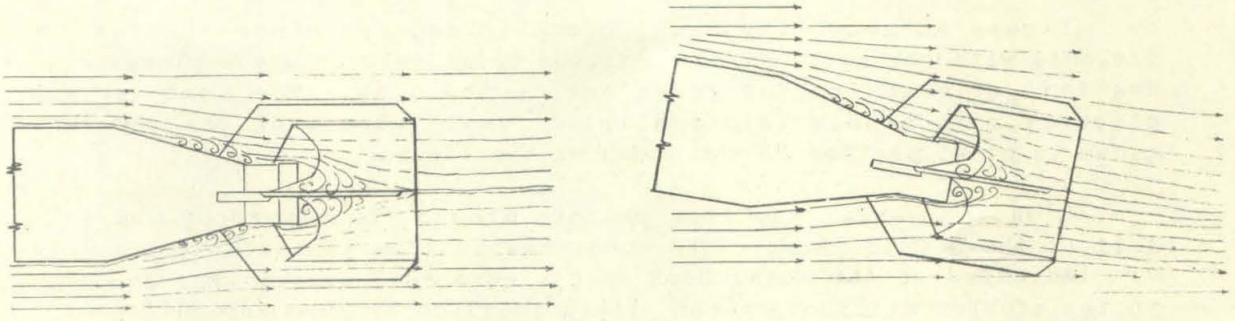

YAW = 0°

YAW = 10°

FIG. 14 – FLOW PATTERNS AT 0° AND 10° YAW AROUND AFTERBODY AND FINS OF M38A2 PRACTICE BOMB

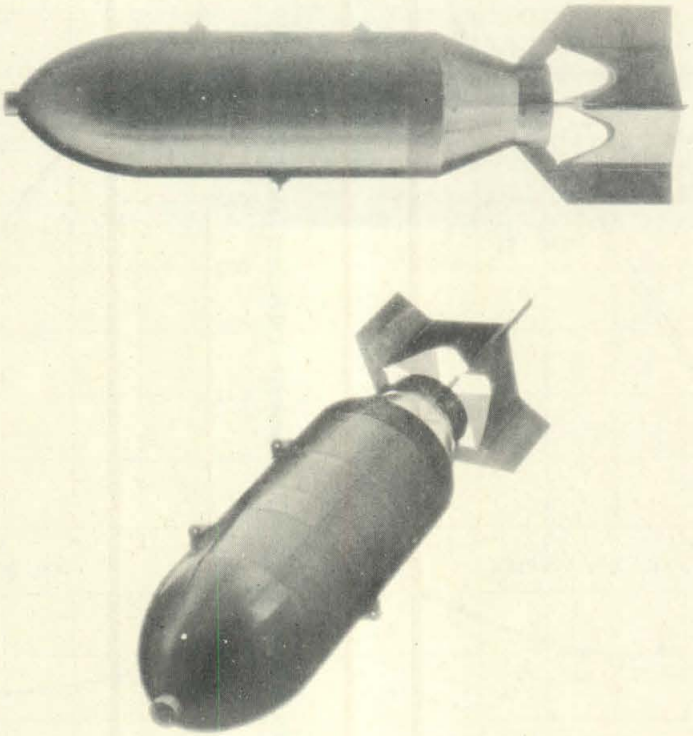

FIG. 15 - MODEL OF AN-M43 G.P. 500 LB. BOMB

AN-M43 G.P. 500 LB. BOMB

This is a general purpose demolition bomb with cylindrical body, ogive nose, and box type tail.

Figure 1 and Table II give the outline and principal dimensions, and photographs of the model are shown in Figure 15.

Figure 16 shows the drag, cross force, and moment coefficients with the tail in two positions relative to the yaw plane. The tail orientation has no effect on the drag. The bomb is slightly more stable (statically) at small yaws when the yaw plane is at 45 degrees to the sides of the fin box.

Figure 17 shows the flow pattern around the afterbody and tail of the 500 lb. Bomb. The same general flow characteristics are indicated on the M38A2 Bomb (see Figure 14), except that due to the steeper afterbody taper, there is slightly more separation along the afterbody just ahead of the tail. This is particularly noticeable in the flow pattern at 10 degrees yaw.

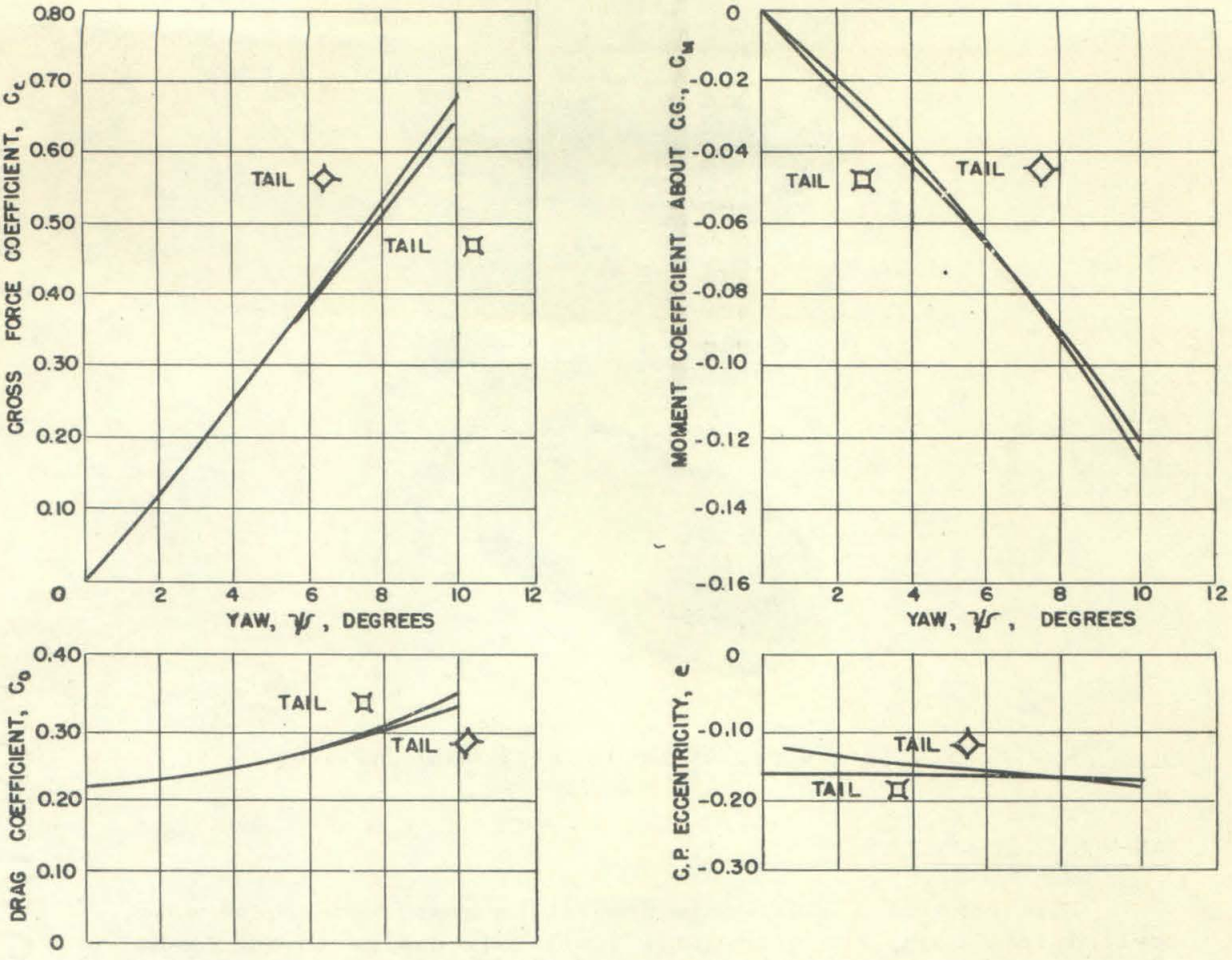

FIG. 16 – AN–M43 G.P. 500 BB. BOMB

FORCE AND MOMENT COEFFICIENTS

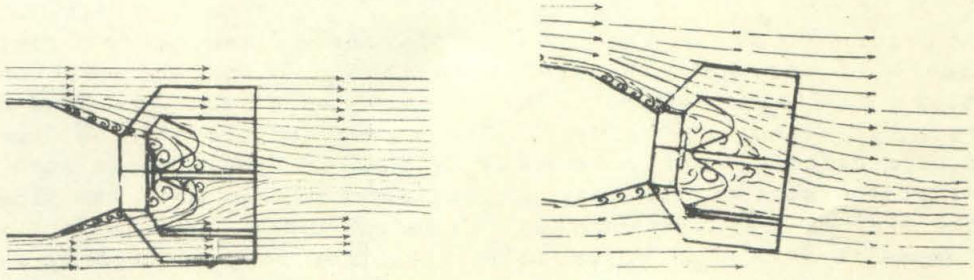

YAW = 0°

YAW = 10°

FIG. 17 – FLOW PATTERNS AT 0° AND 10° YAW ARCUND AFTERBODY

AND FINS OF AN–M43 G.P. 500 LB. BOMB

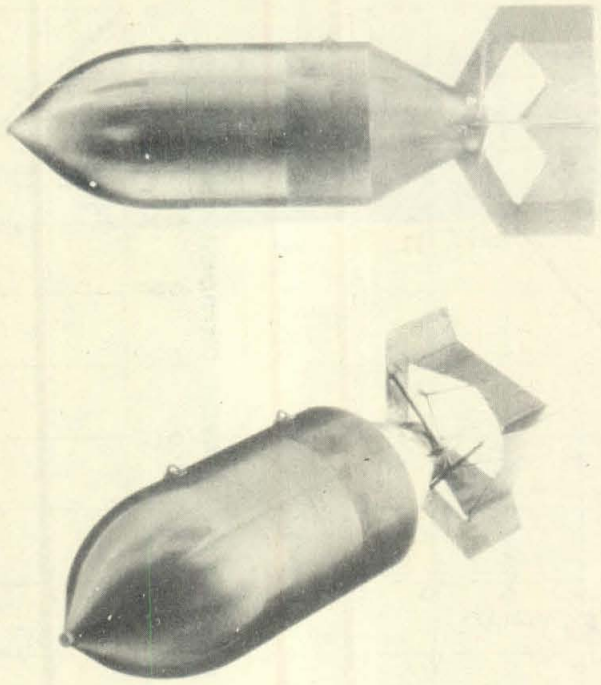

FIG. 18 – MODEL OF AN-M56 L.C. 4000 LB. BOMB

AN-M56 L.C. 4000 LB. BOMB

This bomb is a light case demolition bomb, with ogive nose, cylindrical body, and a box tail similar in design to the AN-M43 500 lb. Bomb and the M38A2 Practice Bomb, except that braces are privided to stiffen the fin box and the fins.

Figure 18 shows two photographic views of the model. The fin braces are clearly indicated.

Figure 19 shows the drag, cross force, and moment coefficients of the 4000 lb. Bomb with the tail in two positions relative to the yaw plane. The orientation of the tail has no appreciable effect on the drag. The moment and cross force, however, are affected very noticeably by the tail position in such a way that the static stability is considerably less when the sides of the fin box are at 45 degrees to the yaw plane. This effect is the opposite from that observed in the other box-tail bombs, and the reason is not apparent, either from the behavior during the force tests or from observation in the Polarized Light Flume.

Figure 20 shows the flow pattern around the afterbody and tail. Due to the sharp taper of the afterbody, there is a wide zone of separation and eddying flow around the afterbody extending into the interior of the fin box. The bluntness of the afterbody probably accounts for the higher drag of this model and also its lower stability as measured by the moment coefficient.

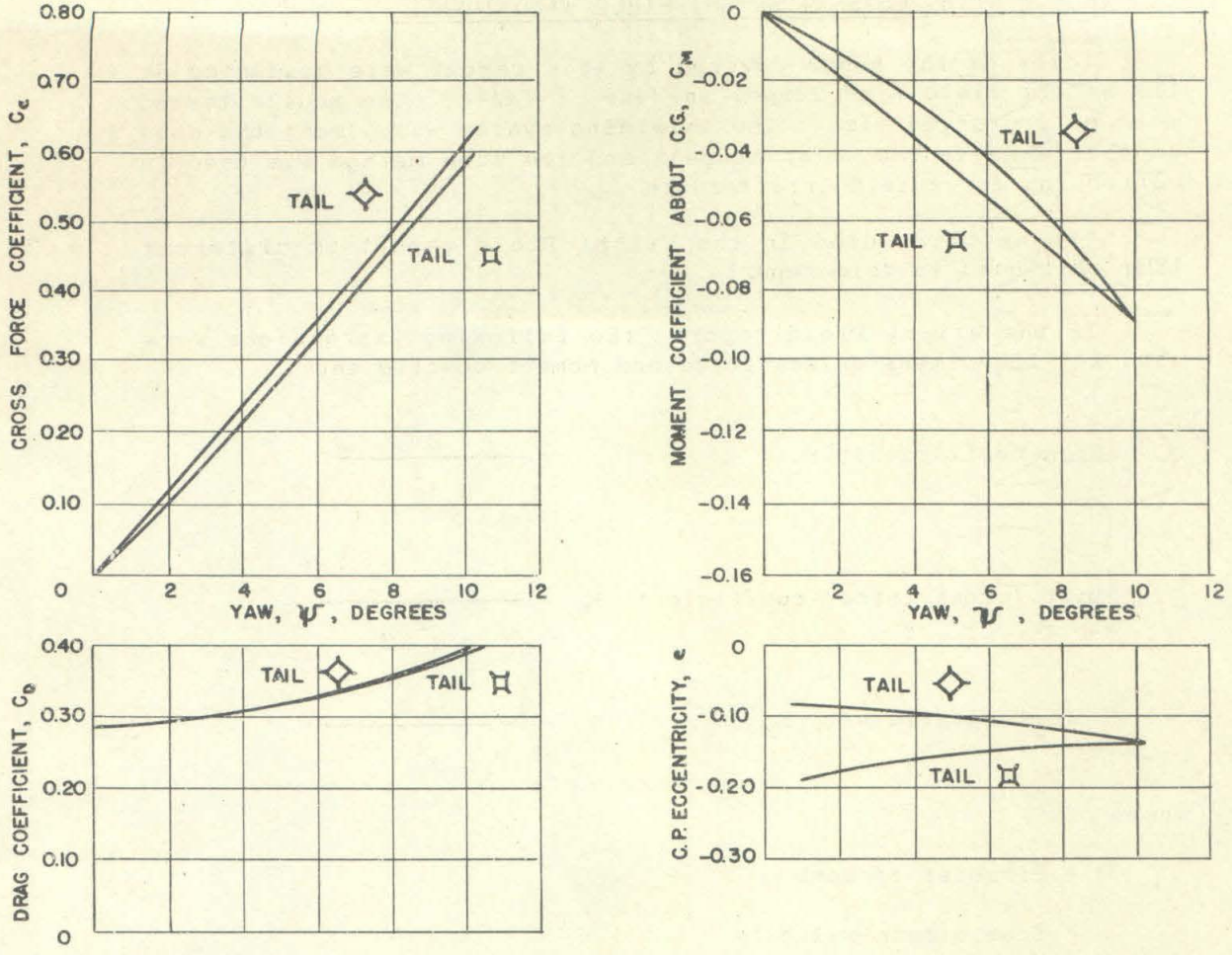

FIG. 19 – AN-M56 L.C. 4000 LB. BOMB

FORCE AND MOMENT COEFFICIENTS

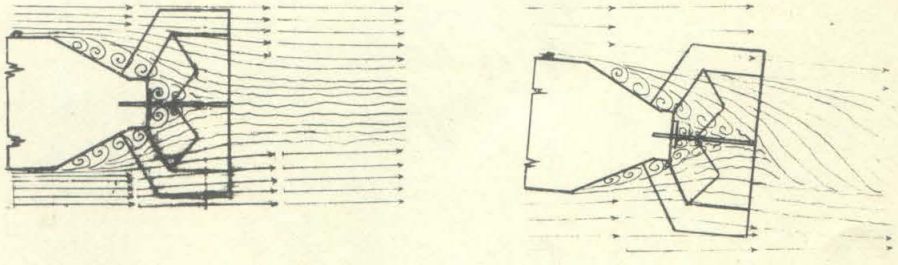

YAW = 0°

YAW = 10°

FIG. 20 – FLOW PATTERNS AT 0° AND 10° YAW AROUND AFTERBODY AND FINS OF AN-M56 L.C. 4000 LB. BOMB

COMPARISON WITH TESTS AT WRIGHT FIELD WIND TUNNEL

Tests of the bombs covered by this report were conducted at the Wright Field Wind Tunnel in June, 1944[1]. The models tested were of prototype size. The shielding system was almost the same as that used in the water tunnel, and the same method was used in correcting for shield interference.

The notation used in the Wright Field report is different from that used in this report.

In the Wright Field report, the following expressions were used for the dimensionless force and moment coefficients:

Drag coefficient, $K_D = \frac{D}{\rho d^2 U}$

Lift (cross force) coefficient, $K_L = \frac{L}{\rho d^2 U^2}$

Moment coefficient, $K_M = \frac{M}{\rho d^3 U^2}$

where

d = diameter of bomb

U = free stream velocity

Comparing the above notation with the notation in the appendix to this report, it is seen that to convert the Wright Field notation to the water tunnel notation, the following transformations are necessary:

$$C_D = \frac{8}{\pi} K_D$$

$$C_C = \frac{8}{\pi} K_L$$

$$C_M = \frac{8d}{\pi I} K_M$$

In order to compare the Wright Field coefficient curves with the curves resulting from the Water Tunnel tests, the Wright Field curves were first corrected for asymmetry, then replotted and faired to represent completely symmetrical projectiles. The resulting comparisons are shown in Figures 21 to 25 for the Concrete Practice Bombs, the 500 lb. Bomb, and the 4000 lb. Bomb. The comparisons are for the same orientation of the tails with respect to the yaw plane.

For the Concrete Practice Bombs the drag shown by the Water Tunnel tests is, near zero yaw, some 50% higher than shown by the

Wright Field tests. The cross force compares reasonably well for all three of the concrete bombs. The moment coefficients, except for the bomb with the CPCA No. tail, do not compare at all closely. The erratic variation of moment near zero yaw, shown by the Wright Field tests, could not be reproduced in the Water Tunnel. On Page 5 of the Wright Field report the authors state that the results obtained on the 100 lb. bombs were not entirely satisfactory.

For the 500 lb. Bomb and the 4000 lb. Bomb the Wright Field tests and the Water Tunnel tests show coefficients that compare quite closely. The drag coefficients are slightly higher in the Water Tunnel, but the moment and cross force coefficients, particularly at small yaws, compare very well.

The Reynolds numbers for the full size models tested in the wind tunnel are from three to twenty times the Reynolds numbers for the small models tested in the water tunnel. The comparison of the Reynolds numbers is shown in Table I. The drag coefficients measured in the water tunnel are about twice as high as have been measured at the same Reynolds number in tests of more fully streamlined shapes of approximately equal dimensions and surface areas. This would indicate that, for the bombs, form drag predominates and only a small decrease in drag could be expected even with a large increase in Reynolds number.

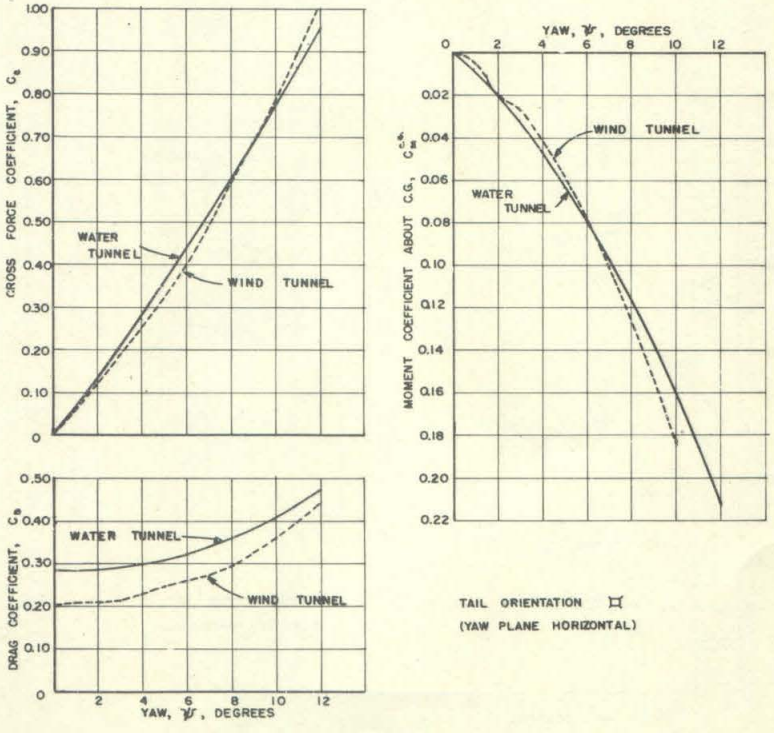

FIG. 21 – COMPARISON OF WATER TUNNEL AND WRIGHT FIELD WIND TUNNEL TESTS
Concrete Practice Bomb with CPCA No. 1 (Large Fin Box) Tail

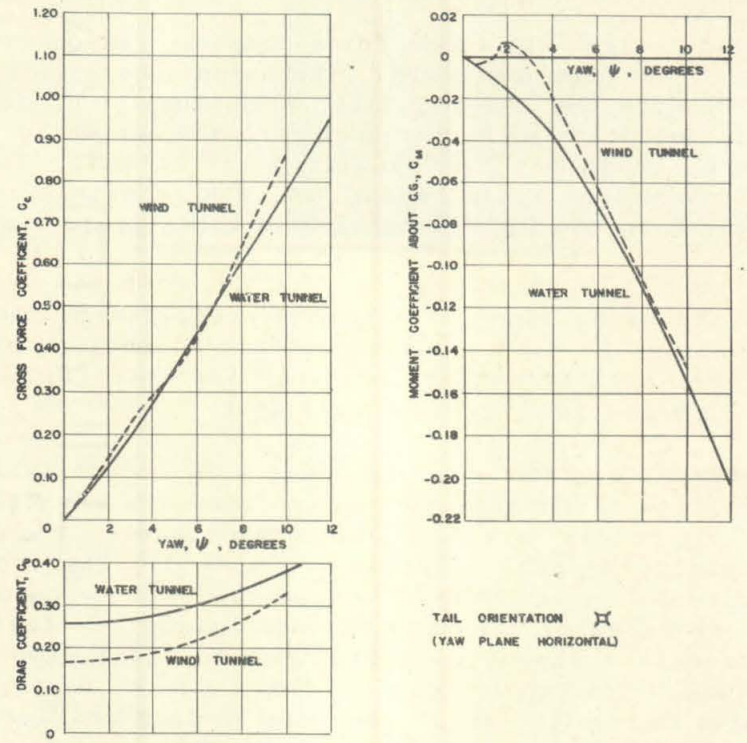

FIG. 22 – COMPARISON OF WATER TUNNEL AND WRIGHT FIELD WIND TUNNEL TESTS
Concrete Practice Bomb with CPCA No. 2 (Small Fin Box) Tail

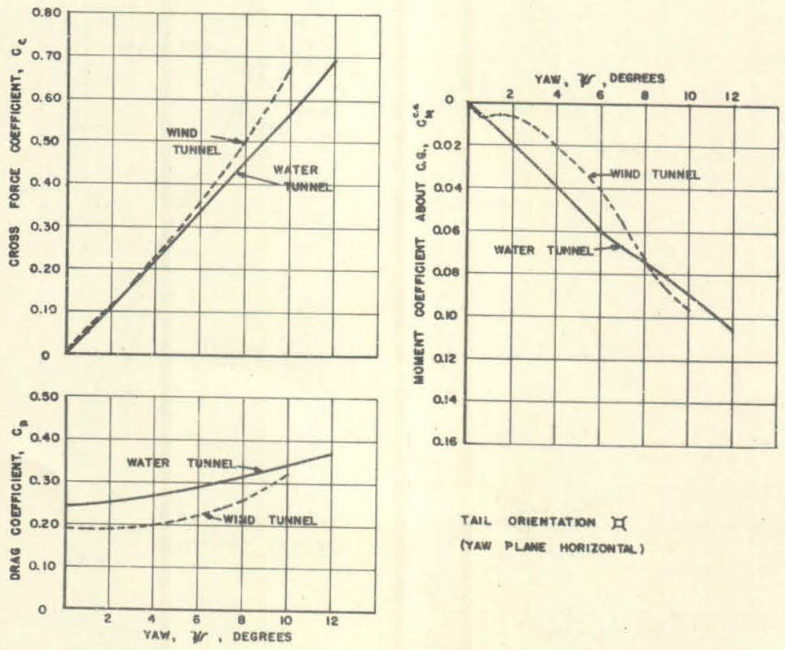

FIG. 23 – COMPARISON OF WATER TUNNEL AND WRIGHT FIELD WIND TUNNEL TESTS
Concrete Practice Bomb with CPCA No. 3 (Drum Type) Tail

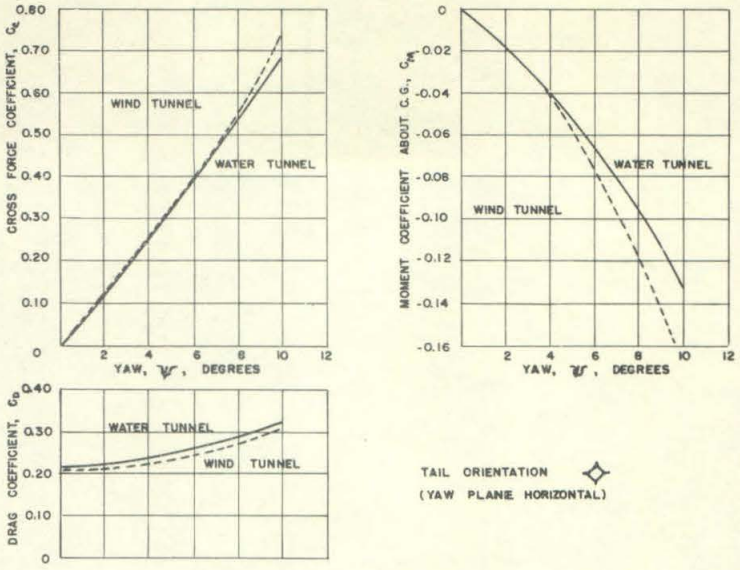

FIG. 24 – COMPARISON OF WATER TUNNEL AND WRIGHT FIELD WIND TUNNEL TESTS
AN–M43 G.P. 500 LB. BOMB

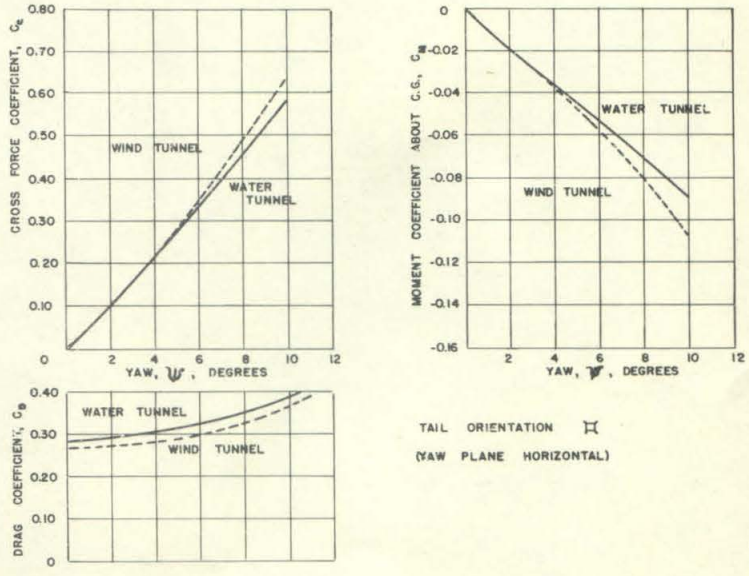

FIG. 25 – COMPARISON OF WATER TUNNEL AND WRIGHT FIELD WIND TUNNEL TESTS
AN–M56 L.C. 4000 LB. BOMB

APPENDIX

DEFINITIONS

YAW ANGLE, ψ

The angle, in a horizontal plane, which the axis of the projectile makes with the direction of motion. Looking down on the projectile, yaw angles in a clockwise direction are positive (+) and in a counterclockwise direction, negative (−).

PITCH ANGLE, α

The angle, in a vertical plane, which the axis of the projectile makes with the direction of motion. Pitch angles are positive (+) when the nose is up and negative (−) when the nose is down.

LIFT, L

The force, in pounds, exerted on the projectile normal to the direction of motion and in a vertical plane. The lift is positive (+) when acting upward and negative (−) when acting downward.

CROSS FORCE, C

The force, in pounds, exerted on the projectile normal to the direction of motion and in a horizontal plane. The cross force is positive when acting in the same direction as the displacement of the projectile nose for a positive yaw angle, i.e., to an observer facing in the direction of travel, a positive cross force acts to the right.

DRAG, D

The force, in pounds, exerted on the projectile parallel with the direction of motion. The drag is positive when acting in a direction opposite to the direction of motion.

MOMENT, M

The torque, in foot pounds, tending to rotate the projectile about a transverse axis. Yawing moments tending to rotate the projectile in a clockwise direction (when looking down on the projectile) are positive (+), and those tending to cause counterclockwise rotation are negative (−). Pitching moments tending to rotate the projectile in a clockwise direction (when looking at the projectile from the port side) are positive (+), and those tending to cause counterclockwise rotation are negative (−).

In accordance with this sign convention a moment has a destabilizing effect when it has the same sign as the yaw angle or pitch angle, and a stabilizing effect when the moment and yaw or pitch angle have opposite signs

NORMAL COMPONENT, N

The sum of the components of the drag and cross force (or lift) acting normal to the axis of the projectile. The value of the normal component is given by the following:

$$N = D \sin \psi + C \cos \psi \qquad (1)$$

or

$$N = D \sin \alpha + L \cos \alpha \qquad (1a)$$

in which

N = Normal component in lbs

D = Drag in lbs

C = Cross force in lbs

L = Lift force in lbs

ψ = Yaw angle in degrees

α = Pitch angle in degrees

CENTER OF PRESSURE, CP

The point in the axis of the projectile at which the resultant of all forces acting on the projectile is applied.

CENTER-OF-PRESSURE ECCENTRICITY, e

The distance between the center of pressure (CP) and the center of gravity (CG) expressed as a decimal fraction of the length (l) of the projectile. The center-of-pressure eccentricity is derived as follows:

$$e = (l_{cp} - l_{cg}) \frac{1}{l} = \frac{1}{l} \frac{M_{cg}}{N} \qquad (2)$$

in which

e = Center-of-pressure eccentricity

l = Length of projectile in feet

l_{cg} = Distance from nose of projectile to CG in feet

l_{cp} = Distance from nose of projectile to CP in feet

COEFFICIENTS

The force and moment coefficients used are derived as follows:

Drag coefficient, $$C_D = \frac{D}{\rho \frac{V^2}{2} A_D} \quad (3)$$

Cross force coefficient, $$C_C = \frac{C}{\rho \frac{V^2}{2} A_D} \quad (4)$$

Lift coefficient, $$C_L = \frac{'L}{\rho \frac{V^2}{2} A_D} \quad (5)$$

Moment coefficient, $$C_M = \frac{M}{\rho \frac{V^2}{2} A_D l} \quad (6)$$

in which

D = Measured drag force in lbs

C = Measured cross force in lbs

'L = Measured lift force in lbs

ρ = Density of the fluid in slugs/cu ft = w/g

w = Specific weight of the fluid in lbs/cu ft

g = Acceleration of gravity in ft/sec^2

A_D = Area in sq ft at the maximum cross section of the projectile taken normal to the geometric axis of the projectile

V = Mean relative velocity between the water and the projectile in ft/sec

M = Moment, in foot-pounds, measured about any particular point on the geometric axis of the projectile

l = Overall length of the projectile in feet

RUDDER EFFECT

The total increase or decrease in moment coefficient, at a given yaw or pitch angle, resulting from a given rudder setting. This increase or decrease in moment coefficient is measured from the moment coefficient curve for neutral rudder setting.

REYNOLDS NUMBER

In comparing hydraulic systems involving only friction and inertia forces, a factor called Reynolds number is of great utility. This is defined as follows:

$$R = \frac{lV}{\nu} = \frac{lV\rho}{\mu} \qquad (7)$$

in which

R = Reynolds number

l = Overall length of projectile, feet

V = Velocity of projectile, feet per sec

ν = Kinematic viscosity of the fluid, sq ft per sec = μ/ρ

ρ = Mass density of the fluid in slugs per cu ft

μ = Absolute viscosity in pound-seconds per sq ft

Two geometrically similar systems are also dynamically similar when they have the same value of Reynolds number. For the same fluid in both cases, a model with small linear dimensions must be used with correspondingly large velocities. It is also possible to compare two cases with widely differing fluids provided l and V are properly chosen to give the same value of R.

CAVITATION PARAMETER

In the analysis of cavitation phenomena, the cavitation parameter has been found very useful. This is defined as follows:

$$K = \frac{P_L - P_B}{\rho \frac{V^2}{2}} \qquad (8)$$

in which

K = Cavitation parameter

P_L = Absolute pressure in the undisturbed liquid, lbs/sq ft

P_B = Vapor pressure corresponding to the water temperature, lbs/sq ft

V = Velocity of the projectile, ft/sec

ρ = mass density of the fluid in slugs per cu ft = w/g

w = weight of the fluid in lbs per cu ft

g = acceleration of gravity

Note that any homogeneous set of units can be used in the computation of this parameter. Thus, it is often convenient to express this parameter in terms of the head, i.e.,

$$K = \frac{h_L - h_B}{\frac{V^2}{2g}} \qquad (9)$$

where

h_L = Submergence plus the barometric head, ft of water

h_B = Pressure in the bubble, ft of water

It will be seen that the numerator of both expressions is simply the net pressure acting to collapse the cavity or bubble. The denominator is the velocity pressure. Since the entire variation in pressure around the moving body is a result of the velocity, it may be considered that the velocity head is a measure of the pressure available to open up a cavitation void. From this point of view, the cavitation parameter is simply the ratio of the pressure available to collapse the bubble to the pressure available to open it. If the K for incipient cavitation is considered, it can be interpreted to mean the maximum reduction in pressure on the surface of the body measured in terms of the velocity head. Thus, if a body starts to cavitate at the cavitation parameter of one, it means that the lowest pressure at any point on the body is one velocity head below that of the undisturbed fluid.

The shape and size of the cavitation bubbles for a specific projectile are functions of the cavitation parameter. If p_B is taken to represent the gas pressure within the bubble instead of the vapor pressure of the water, as in normal investigations, the value of K obtained by the above formula will be applicable to an air bubble. In other words, the behavior of the bubble will be the same whether the bubble is due to cavitation, the injection of exhaust gas, or the entrainment of air at the time of launching.

The cavitation parameter for incipient cavitation has the symbol K_i.

The following chart gives values of the cavitation parameter as a function of velocity and submergence in sea water.

GENERAL DISCUSSION OF STATIC STABILITY

Water tunnel tests are made under steady flow conditions, consequently the results only indicate the tendency of the steady state hydrodynamic couples and forces to cause the projectile to return to or move away from its equilibrium position after a

disturbance. Dynamic couples and forces including either positive or negative damping are not obtained. If the hydrodynamic moments are restoring the projectile, then it is said to be statically stable, if nonrestoring, statically unstable. In the discussion of static stability the actual motion following a perturbation is not considered at all. In fact, the projectile may oscillate continuously about an equilibrium position without remaining in it. In this case it would be statically stable, but would have zero damping and hence, be dynamically unstable. With negative damping a projectile would oscillate with continually increasing amplitude following an initial perturbation even though it were statically stable. Equilibrium is obtained if the sum of the hydrodynamic, buoyant, and propulsive moments equal zero. In general, propulsive thrusts act through the center of gravity of the projectile so only the first two items are important.

If a projectile is rotating from its equilibrium position so as to increase its yaw angle positively, the moment coefficient must increase negatively (according to the sign convention adopted) in order that it be statically stable. Therefore, for projectiles without controls or with fixed control surfaces, a negative slope of the curve of moment coefficient vs yaw gives static stability and a positive slope gives instability. For a projectile without controls, static stability is necessary for a successful flight unless stability is obtained by spinning as in the case of rifle shells. For a projectile with controls, stabilizing moments can be obtained by adjusting the control surfaces, and the slope of the moment coefficient, as obtained with fixed rudder position, need not give static stability. Where buoyancy either acts at the center of gravity or can be neglected, equilibrium is obtained when the hydrodynamic moment coefficient equals zero. For symmetrical projectiles this occurs at zero yaw angle, i.e., when the projectile axis is parallel to the trajectory. For nonsymmetrical projectiles, such as a torpedo when the rudders are not neutral, the moment is not zero at zero yaw but vanishes at some definite angle of attack. Where buoyancy cannot be neglected equilibrium is obtained when $C_M = -C_{Buoyancy}$, and the axis of the projectile is at some angle with the trajectory.

For symmetrical projectiles the degree of stability or instability can be obtained from the center-of-pressure curves. If the center of pressure falls behind the center of gravity, a restoring moment exists giving static stability. If the center of pressure falls ahead of the center of gravity, the moment is nonrestoring, and the projectile will be statically unstable. The degree of stability or instability is indicated approximately by the distance between the center of gravity and the center of pressure. In general, for nonsymmetrical projectiles, the cross force or lift is not zero when the moment vanishes so that the center of pressure curve is not symmetrical and the simple rules just stated cannot be used to determine whether or not the projectile will be stable. In such cases careful interpretation of the moment curves is a more satisfactory method of determining stability relationship.

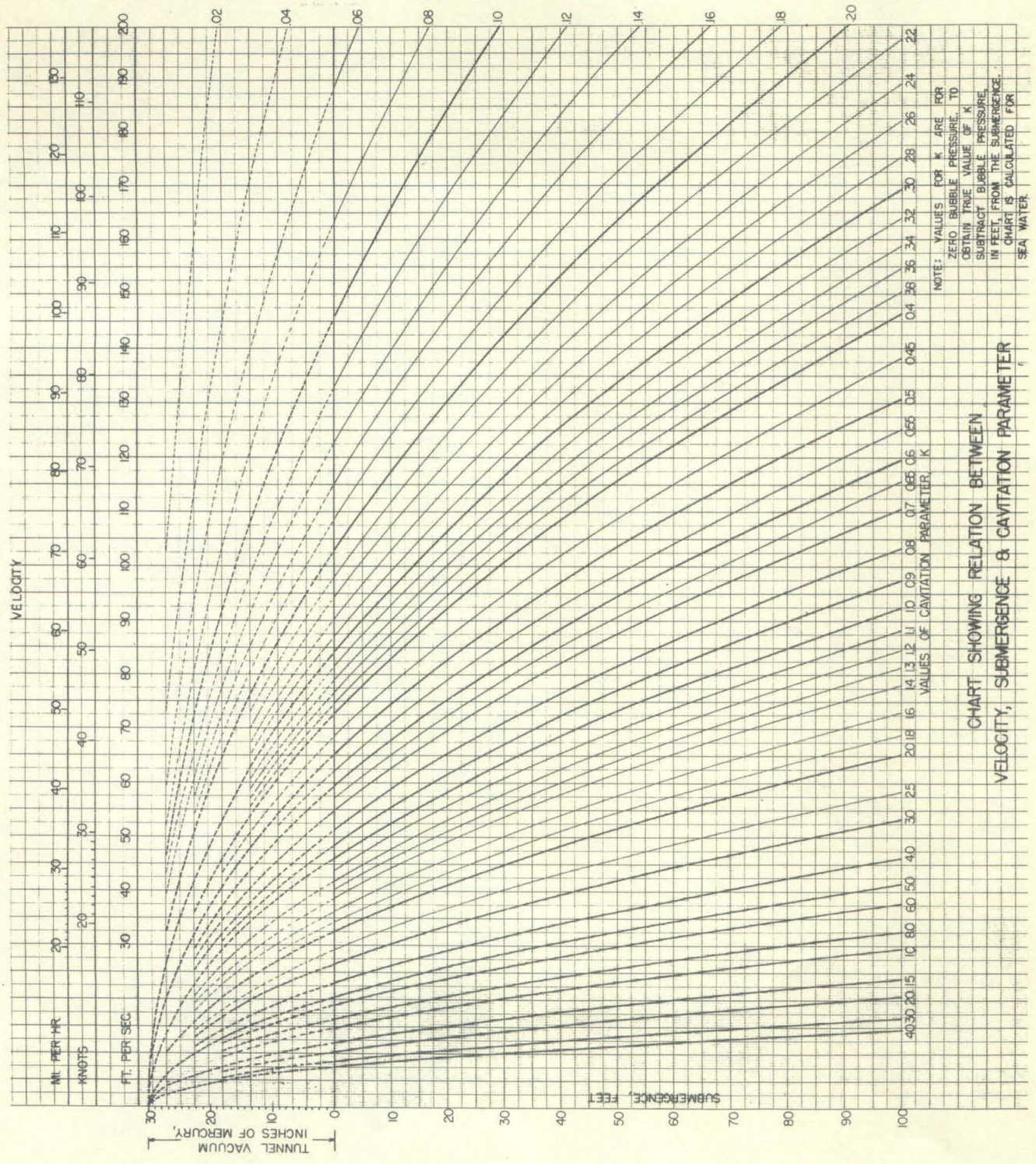
CHART SHOWING RELATION BETWEEN
VELOCITY, SUBMERGENCE & CAVITATION PARAMETER
NOTE: VALUES FOR K ARE FOR ZERO BUBBLE PRESSURE. TO OBTAIN TRUE VALUE OF K SUBTRACT BUBBLE PRESSURE, IN FEET, FROM THE SUBMERGENCE. CHART IS CALCULATED FOR SEA WATER.
VELOCITY
NAUT. MI. PER HR.
KNOTS
FT. PER SEC.
VALUES OF CAVITATION PARAMETER, K
SUBMERGENCE, FEET
TUNNEL VACUUM
INCHES OF MERCURY,